

# Influence of PEDOT:PSS buffer layer on the performance of organic photocoupler\*

WANG Zhong-qiang (王忠强)<sup>1</sup>, WU Xiao-ming (吴晓明)<sup>1</sup>, JING Na (荆娜)<sup>1</sup>, HOU Qing-chuan (侯庆传)<sup>1</sup>, Hu Zi-yang (胡子阳)<sup>1</sup>, CHENG Xiao-man (程晓曼)<sup>1</sup>, HUA Yu-lin (华玉林)<sup>1</sup>, WEI Jun (魏军)<sup>1,2</sup>, and YIN Shou-gen (印寿根)<sup>1\*\*</sup>

1. Key Laboratory on Display Materials and Photoelectric Devices of Education Ministry of China, Institute of Material Physics, Tianjin Key Laboratory for Photoelectric Materials and Devices, Tianjin University of Technology, Tianjin 300384, China

2. Singapore Institute of Manufacturing Technology, 71 Nanyang Drive, Singapore

(Received 17 February 2009)

We have fabricated an organic photocoupler with organic light-emitting diodes (OLEDs) with 520 nm emissive wavelength as the input light source and a photodiode (PD) based on poly(3-hexylthiophene) (P3HT):1-(3-methoxycarbonyl)propyl-1-phenyl-(6,6)-C<sub>61</sub> (PCBM) as the detector. The influences of buffer layer (PEDOT:PSS) on output current ( $I_{out}$ ), current transfer ratio (CTR) and time response characteristics of the photocoupler device were studied. Through our experiments, It is found that the output current linearly increases with the input current, the max output current and CTR of the devices with PEDOT:PSS buffer layer are 2 times and 7 times than that of the devices without buffer layer respectively, which show that the existence of buffer layer can enhance the output photocurrent efficiently. Moreover, the existence of PEDOT:PSS eliminates the time delay of the devices.

**Document code:** A **Article ID:** 1673-1905(2009)03-0173-4

**DOI** 10.1007/s11801-009-9031-9

Organic electronic and optoelectronic devices have attracted more and more attention because of their light weight, low cost, and potential for large area devices<sup>[1-4]</sup>. In recent years many types of organic electronic and optoelectronic devices have got commercial availability, which made the organic electronics and devices become quite active. Since the efficiency of the organic light emitting diodes(OLEDs) was highly improved by C. W. Tang in 1987<sup>[5]</sup>, the performance of OLEDs has made great progress in the past decade years<sup>[6-8]</sup>. Meanwhile, organic polymeric bulk heterojunction photovoltaic materials and devices (OPVs) have been developed so fast in recent years, and the highest efficiency of OPVs has reached 6.5%<sup>[9]</sup>. So it is possible to fabricate an organic photocoupler with OLEDs as the input unit and OPVs as the output unit connected by insulator layer.

A photocoupler is a functional device that uses a short optical transmission path to transfer a signal between elements of a circuit, while keeping electrical signal isolated<sup>[10,11]</sup>. This merit could improve the anti-jamming ability of integrated circuit. It is widely used in microelectronic technologies. Compared with the inorganic photocoupler, the organic

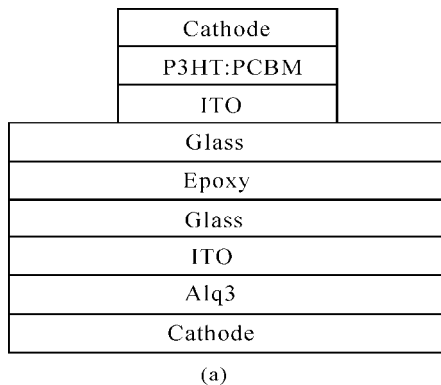
photocoupler has many advantages, such as light weight, low cost, flexibility et al. Up to now, few research groups engage this job<sup>[6,12]</sup>. In this paper, an organic photocoupler device composed of an OLED and an OPV unit is constructed, with 520 nm OLED emissive light wavelength as the input light and the P3HT:PCBM bulk heterojunction active layer as the output detector respectively. In order to research the influence of buffer layer we have fabricated devices D1 (the output unit without PEDOT:PSS buffer layer) and D2 (the output unit with PEDOT:PSS buffer layer). Through our experiments we have found that the max output current of D2 is as 2 times as that of D1, the CTR of D2 is as 7 times as that of D1. Meanwhile D2 has quicker speed to respond the input signal than D1.

In order to investigate the influence of a buffer layer, it is necessary to fabricate an input light device with stable performance. From our previous work in OLEDs<sup>[13-15]</sup>, we fabricated the OLED light emissive devices with the structure of ITO/NPB(40 nm)/Alq<sub>3</sub>(70 nm)/LiF(0.8 nm)/Al(120 nm) with 520 nm emissive wavelength. An active photodiode material should have the following characteristics: high photon-to-

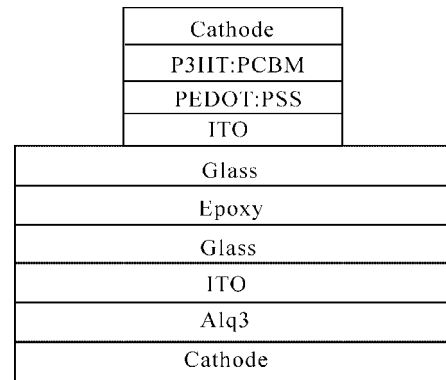
\* This work has been supported by the National Natural Science Foundation of China (60676051, 60876046), Tianjin Natural Science Foundation (06TXJJJC14603, 07JCYBJC12700) and the Tianjin Key Discipline of Material Physics and Chemistry.

\*\* E-mail: sgyin@tjut.edu.cn.

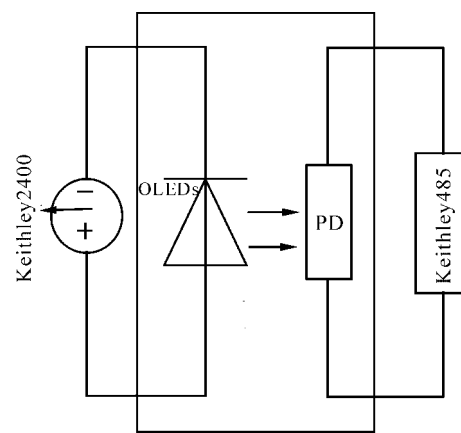
charge carrier branching ratio, high carrier mobility, fast electron transfer ability from charge donor to acceptor. At present, the P3HT:PCBM blending film is the best choice for a photodiode because the output characteristic of the device based on P3HT:PCBM has faster time response to the input light [16] and the highest efficiency achieved in OPVs is based on a P3HT:PCBM bulk heterojunction [17]. Many factors influence the performance of a photodiode (PD), such as the molecular weight of P3HT, blend composition, annealing and film deposition. Hence our output unit of PD was prepared according to the following steps: the pre-cleaned ITO glass ( $10\Omega/\square$ ) was used as the substrate. PEDOT:PSS film of D2 was spun cast at 1000 rpm for 20 s, then annealed at 100 °C for 10 min. The active layer was spun cast from a blend solution of P3HT and PCBM (1:1 weight ratio, P3HT concentration=20 mg/ml) at 1000 rpm for 40 s, then covered with a Petri dish and dried at 180 °C for 20 min in the Argon atmosphere. At last, the LiF/Al electrodes with the thickness of 0.8/120 nm were deposited subsequently by thermal evaporation to construct the PD unit of D1 (ITO/P3HT:PCBM/LiF/Al) and D2 (ITO/PEDOT:PSS/P3HT:PCBM/LiF/Al) respectively. Finally, the input unit (OLED) and output unit (PD) were glued together by index matching epoxy carefully to form an integrated photocoupler, as depicted in Fig.1(a) and (b). The active layer area of OLED and PD was  $0.3\text{ cm}^2$  and  $0.15\text{ cm}^2$  ( $S_{\text{OLED}}:S_{\text{PD}} = 2:1$ ) respectively. Their corresponding equivalent circuit of the organic photocoupler was illustrated in Fig.1(c). The  $I_{\text{out}}$  versus  $I_{\text{in}}$ , CTR versus  $I_{\text{in}}$  and time response characteristics were recorded simultaneously with the measurement using a Keithley model 2400 programmable voltage–current source. The EL spectrum of OLED was measured by F-4500 fluorescence spectrophotometer. The absorption spectrum of P3HT:PCBM was measured by UV: JASCOV-570. All the measurements were carried out at room temperature in air without any device encapsulation and protection of inert gases.



(a)



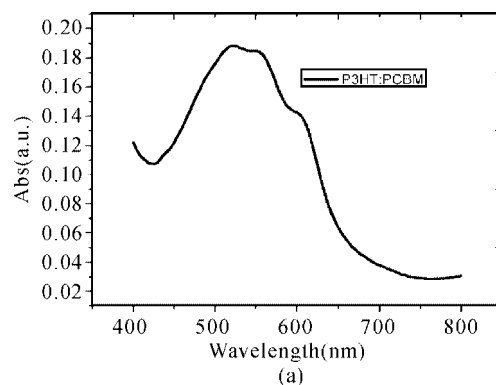
(b)



(c)

**Fig.1 (a) and (b) The configurations of the D1 and D2 respectively, and (c) the corresponding measurement circuit.**

Fig.2 (a) is the absorption spectrum of P3HT:PCBM film that shows the main absorption wavelengths of P3HT:PCBM active film covering from 460 nm to 630 nm region and the sharp absorption is at 517 nm. So the OLED with emissive wavelength 520 nm was chosen. For the good performance (stability, color purity et.al) of OLED, the thickness of functional layer and cathode were well-controlled based on our previous experience on the fabrication of OLEDs [10-13], the EL spectrum is illustrated in Fig.2 (b).



(a)

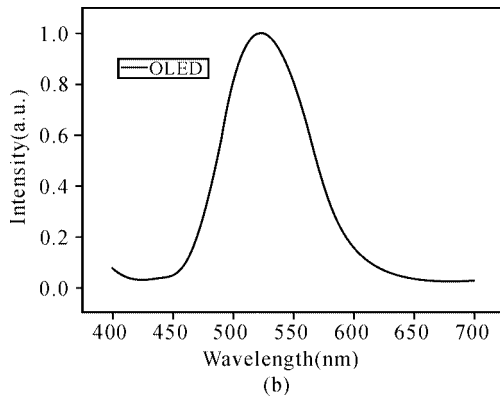


**Fig.2 (a) The absorption of P3HT:PCBM, (b) The EL spectrum of OLED.**

Light-induced current ( $I_{out}$ ), CTR ( $I_{out}/I_{in}$ ) and time response, which reflect the performance of the photocoupler, are important in the context of the application in integrated circuit. Fig.3(a) shows the curve of  $I_{out}$  versus  $I_{in}$  (the input current of OLED) and Fig.3(b) depicts the variation of CTR with input current ( $I_{in}$ ). In Fig.3(a), the output currents of both D1 and D2 ( $I_{out}$ , the current passing out the photodiodes) are positively proportional to the input current ( $I_{in}$ , the cur-

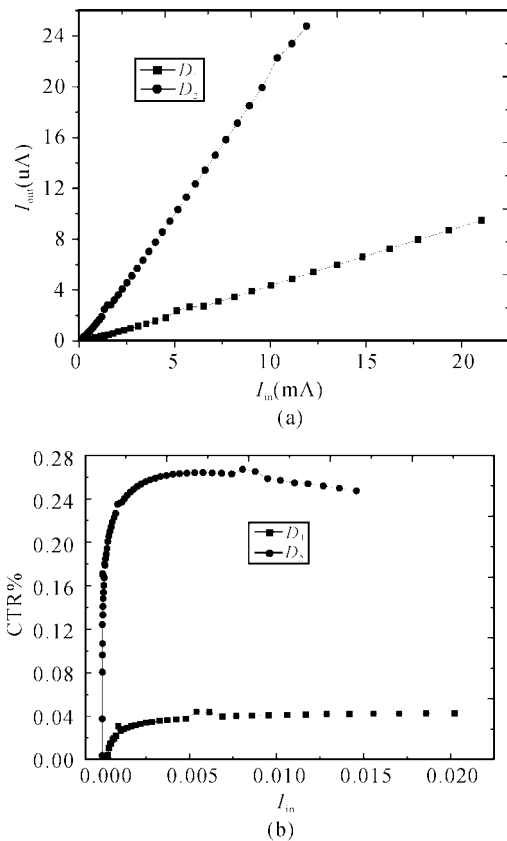


**Fig.3.(a)  $I_{out}$ - $I_{in}$  characteristic,  $I_{out}$  is the current through the PD,  $I_{in}$  is the input current of OLED, (b) current transfer ratio (CTR (defined as  $I_{out}/I_{in}$ )) -  $I_{in}$ .**

rent injecting into the OLED), which indicates that the  $I_{out}$  enhances nearly linear with the increasing of  $I_{in}$ . Moreover, the  $I_{out}$  of D2 is nearly as 5 times as that of D1 at  $I_{in}$  of 5.0 mA, the maximum CTR of D2 is as 7 times as that of D1. In conclusion, D2 behaves much better performance than that of D1 in  $I_{out}$  property.

Fig.4(a) and (b) reflect the time response characteristics of D1 and D2. In Fig.4. the voltage is the driving voltage of OLED, and the delay is the time duration of each voltage. Through the Fig.4(a) we have found that the output current of D1 increases with the time delay. But we get reversed result in the Fig.4(b). In normal situation, the output current should be similar with Fig.4(b) because of the attenuation of luminous intensity. The result of Fig.4(a) implies that some charges counteract the output current attenuation caused by OLED.

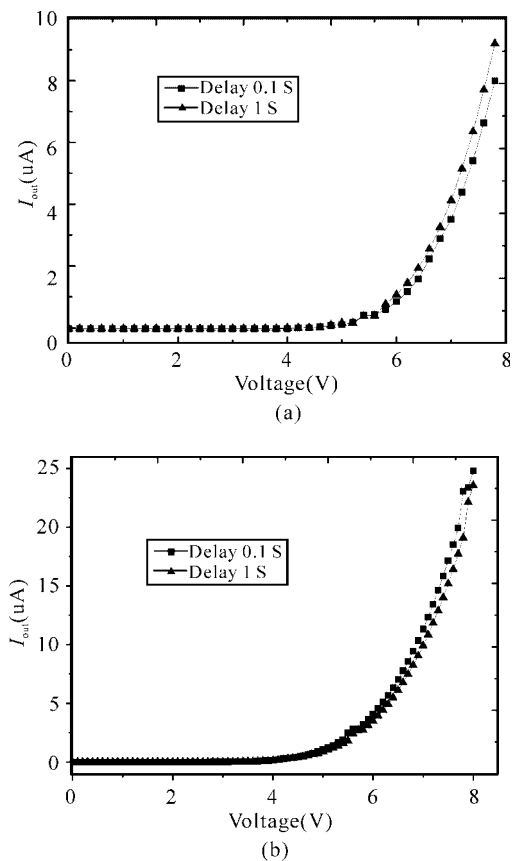


**Fig.4(a) and (b) The time response characteristics of D1 and D2 respectively. ( $I_{out}$  is the output current of device, voltage is the driving voltage of OLED).**

For organic semiconductors, the principal photoinduced charge mechanisms involve the generating of the excitons (electron-hole pairs) at the active heterojunction, then the subsequent processes of charge diffusion and collection<sup>[18]</sup>. However, excitons wouldn't change into photocurrent to-

tally because that the dissociation and recombination of excitons are competing processes drastically<sup>[19]</sup>. As the input light is applied to the active layer P3HT:PCBM, a bound electron-hole pair or exciton is formed. These excitons are strongly bound by Coulomb interaction because of the low dielectric constant of the organic materials<sup>[20]</sup>. In order to achieve photocurrent, the bound electron-hole pairs must dissociate into free charge carriers and immediately move to the electrodes under the influence of the electric field before the recombination processes take place<sup>[21]</sup>. In device D1 the relatively low work function of ITO results in increased series resistance in the device through a reduced rate of hole transfer between ITO and the organic film<sup>[22]</sup>. Meanwhile, charge carriers would be trapped at the interfaces. This large amount of trapped charge carriers will influence the interface properties such as semiconductor band bending and charge carrier generation<sup>[23]</sup>. The higher output current and CTR observed in D2 using chemically modified interfaces are attributed to better wettability of the organic layers compared with the polar ITO surface, and also enhanced charge transfer between the ITO anode and P3HT:PCBM layers by means of the intermediate PEDOT:PSS layer. As a result, the output current of D2 is improved. In device D1 the trapped charge carriers could counteract the output current attenuation. Then, the higher the output current, the longer the time delay. But in device D2 the concentration of trapped charge carriers reduces because of the enhanced charge transfer ratio. So the output current becomes lower with a longer time delay. The result of D2 has shown that the injected current density increases when the interfacial energy step ( $\Delta E$ ) is decreased through modification of the anode work function.  $\Delta E$  is defined as  $\Delta E = U_{\text{Anode}} - E_{\text{HOMO}}$ , where  $E_{\text{HOMO}}$  is the highest occupied molecular orbital (HOMO) energy level of the donor organic layer (4.9 eV for P3HT). At last, we know that the PEDOT:PSS buffer layer not only improves the value of output current and CTR but also eliminates the time delay of device through changing the interfacial energy.

We have investigated the influence of PEDOT:PSS buffer layer on the performance of photocoupler device. Through our experiments we have found that the organic photocoupler's output current is linearly increasing with the input current, and the time delay is eliminated through interfacial modification. Meanwhile, our results show that the organic photocoupler has comparable performance to inorganic photocoupler through choosing suitable material of active layer and compatible interfacial modification material. It would be used in the full organic optoelectronic integrated circuits because of the good performance in future.

## References

- [1] A. J. Heeger, *Angew. Semiconducting and Metallic Polymers: Chem. Int. Ed.*, **40** (2001), 2591.
- [2] F. Padinger, R. S. Rittberger, and N. S. Sariciftci, *Adv. Funct. Mater.*, **13** (2003), 85.
- [3] Holger Spanggaard, and Frederik C. Krebs, *Sol. Energy Mater. Sol. Cells*, **83** (2004), 125.
- [4] S.E. Shaheen, D.S. Ginley, G.E. Jabbour (Eds.), *Special Issue: Organic-based Photovoltaics*, *MRS Bull*, 2005.
- [5] C. W. Tang and S.A Vanslyke, *Appl. Phys. Lett.* **51** (1987), 9135.
- [6] G. F. Dong, Y. Hu, and C. G. Jiang, *Appl. Phys. Lett.*, **88** (2006), 051.
- [7] GAO Zhi-xiang, HAO Yu-ying, and MA Chen, *Journal of Optoelectronics • Laser*, **19** (2008), 152.(in Chinese)
- [8] Y. Wang, Y. L. Hua, and X. M. Wu, *Organic Electronics*, **9** (2008), 692.
- [9] Jin Young Kim, Kwanghee Lee, and Nelson E. Coates, *Science*, **317** (2007), 222.
- [10] U. Tietze, C. Schenk, and E. Schmid. *Electronic Circuits: Design and Application*, Springer, Berlin, 1991, 99.
- [11] S. Gage, D. Evans, M. Hodapp, *Electronic Circuits: Design and Application*, McGraw-Hill, New York, 1977.
- [12] Y. Yao, Hsiang-Yu Chen, and J. S. Huang, *Appl. Phys. Lett.* **90** (2007), 053509.
- [13] Y. Wang, Y. L. Hua, and X.M. Wu, *Appl. Phys. Lett.*, **92** (2008), 123.
- [14] Y. Wang, Y. L. Hua, and X. M. Wu, *Organic Electronics.*, **9** (2008), 273.
- [15] Y. Wang, Y. L. Hua, and X. M. Wu, *Appl. Phys. Lett.*, **93** (2008), 113.
- [16] P. Parkinson, J. Lloyd-Hughes, and M. B. Johnston, *Phys. Rev. B*, **78** (2008), 115321.
- [17] Paul D. Cunningham and L. Michael Hayden, *J. Phys. Chem. C*, **112** (2008), 7928.
- [18] G. Yu, J. Gao, J. C. Hummelen, and F. Wudl, *Science*, **270** (1995), 1789.
- [19] Matthew T. Lloyd, Yee-Fun Lim, and George G. Malliaras, *Appl. Phys. Lett.*, **92** (2008), 143308.
- [20] Tobat P.I. Saragi, Robert Pudzich, and Thomas Fuhrmann-Lieker, *Optical Materials*, **29** (2007), 879.
- [21] Florent Monestier, Jean-Jacques Simon, Philippe Torchio, *Solar Energy Materials & Solar Cells.*, **91** (2007), 405.
- [22] Saghar Khodabakhsh, Brett M. Sanderson, and Jenny Nelson, *Adv. Funct. Mater.*, **16** (2006), 95.
- [23] K. Vandewal, L. Goris, I. Haeldermans, *Thin Solid Films*, **516** (2008), 7135.